Available online at www.sciencedirect.com
SCIENCE DIRECT®
Optical Materials 27 (2004) 619–624
OPTICAL Materials
www.elsevier.com/locate/optmat

Spatial anisotropy of photoelastic and acoustooptic properties in β-BaB_2O_4 crystals

A.S. Andrushchak [a], Y.V. Bobitski [b], M.V. Kaidan [a], B.V. Tybinka [a], A.V. Kityk [c,e,*], W. Schranz [d]

[a] *Lviv Politechnic National University, S. Bandery Street 12, 79013 Lviv, Ukraine*
[b] *Institute of Technics, Rzeszow University, ul. Rejtana 16A, 35-959 Rzeszow, Poland*
[c] *Institute for Computer Science, Technical University of Czestochowa, Al. Armii Krajowej 17, 42-200 Czestochowa, Poland*
[d] *Institut für Experimentalphysik, Universität Wien, Strudlhofgasse 4, A-1090 Wien, Austria*
[e] *Economics and Management Department, Polonia University in Czestochowa, 42-200 Czestochowa, Poland*

Received 6 May 2004; accepted 10 August 2004

Abstract

The paper deals with the spatial anisotropy of photoelastic and acoustooptical properties in β-BaB_2O_4 (BBO) crystals. Our method is based on the construction and analysis of the indicative surfaces describing the spatial anisotropy of the longitudinal and transverse photoelastic effects. By means of the stereographic projections we have determined the maximum values of photoelastic interaction and the anisotropy power. Having the complete photoelastic tensor we calculated the effective photoelastic constant p_{ef} and the efficiency of isotropic and anisotropic acoustooptical diffractions (the figure of merit M) for different geometries of acoustooptical interactions. The most optimal sample geometries suitable for acoustooptical applications were determined within the computer simulations based on the optimization procedure, namely we have found the sample geometries characterizing by the maximal efficiency for the isotropic ($M = 6.3 \times 10^{-15}$ s^3/kg) and anisotropic ($M = 40 \times 10^{-15}$ s^3/kg) diffractions. Taking into account that BBO is known as a rather strong radiation-steady crystal it may be considered as new efficient acoustooptical material for applications in optical systems with superpower laser irradiation.

PACS: 42.25.Hz; 42.70.Mp; 78.20.Hp; 78.20.Fm
Keywords: β-BaB_2O_4 crystals; Photoelastic effect; Spatial anisotropy and indicative surfaces, Figure of merit

1. Introduction

The beta barium borate (BBO) β-BaB_2O_4 crystals are known as efficient materials for non-linear optics applications [1,2]. In our previous papers [3–5] we reported the piezooptical properties of these crystals. The results of these investigations indicate that BBO crystals can be considered also as perspective materials for acoustooptical applications. In this respect further analysis of the photoelastic anisotropy as well as the determination of the figure of merit in BBO seems to be rather actual.

The present paper deals with the spatial anisotropy of photoelastic effect in BBO single crystals. The main purpose of such a study is to determine the geometry of the most effective acoustooptical interaction, i.e., the crystallographic directions for interacting acoustic and optical waves, which are characterized by maximal magnitude of the figure of merit.

* Corresponding author.
E-mail addresses: kityk@ap.univie.ac.at, kityk@el.pcz.czest.pl (A.V. Kityk).

0925-3467/$ - see front matter © 2004 Elsevier B.V. All rights reserved.
doi:10.1016/j.optmat.2004.08.075

2. Calculation of the photoelastic tensor constants

The magnitudes of the piezooptical tensor constants π^D_{im} (at constant electric displacement D) of BBO crystals have been reported in our recent publications [3–5]. Using these data the piezooptical constants π^E_{im} (at constant electric displacement E) can be calculated according to the relation for non-centrosymmetric uniaxial crystals [4,6]

$$\pi^E_{im} \equiv \pi^E_{\lambda\mu\eta\nu} = \pi^D_{\lambda\mu\eta\nu} - r_{\lambda\mu\tau}d_{\tau\eta\nu}/(\varepsilon_o(\varepsilon_{\tau\tau} - 1)) = \pi^D_{\lambda\mu\eta\nu} - \Delta_{\lambda\mu\eta\nu}, \quad (1)$$

where the second term $\Delta_{\lambda\mu\eta\nu}$ is the secondary electrooptic contribution, $r_{\lambda\mu\tau}$ and $d_{\tau\eta\nu}$ are the tensor constants corresponding to the linear electrooptic and piezoelectric effects, respectively, $\varepsilon_0 = 8.85 \times 10^{-12}$ F/m, $\varepsilon_{\tau\tau}$ is the tensor of dielectric constants. For the determination of π^E_{im} the following values have been used: $r_{113} = 0.27$, $r_{222} = -2.41$, $r_{333} = 0.29$, $r_{131} = 1.7$ and $d_{311} = -1.17$; $d_{222} = 2.30$; $d_{333} = 3.4$; $d_{113} = -9.6$ (all values are in 10^{-12} m/V [7]); $\varepsilon_{11} = \varepsilon_{22} = 6.7$ and $\varepsilon_{33} = 8.1$ [8]. The photoelastic tensor constants p^E_{in} are then expressed as [4,6]:

$$p^E_{in} = \pi^E_{im}C_{mn} = \pi^E_{im}S^{-1}_{mn}, \quad (2)$$

where C_{mn} is the elastic constant matrix and S_{mn} is the elastic compliance matrix. Our estimations show that the piezoelectric contribution to the elastic compliances of BBO crystals is less than 1% thereby it can be neglected and we will consider that $S^D_{mn} = S^E_{mn}$. For the calculation of the photoelastic constant p^E_{in} the magnitudes of elastic compliances S_{mn} are taken from [8], excepting S_{14} only. The value of this constant is known from our previous experimental measurements [4]. Table 1 lists the calculated values of π^E_{im} and p^E_{in} constants of BBO crystals as for the temperature of 20 °C and the He–Ne laser wavelength $\lambda = 632.8$ nm.

As one can see seen the BBO have rather large magnitudes of photoelastic constants, especially p_{11} and p_{12}. These crystals have an advantage on such known acoustooptic materials as $LiNbO_3$ or TeO_2 and their photoelastic constants are comparable with corresponding coefficients of fused quartz [9].

Table 1
The average values of piezooptic constants π^D_{im} [3,4], elastic compliance coefficients S_{mn} [6], and calculated values of piezooptic π^E_{im}, and photoelasic p^E_{in} constants of BBO crystal (as for $T = 20$ °C and $\lambda = 632.8$ nm)

Index *im* or *in*	π^D_{im}, Br = 10^{-12} m^2/N	π^E_{im}, Br	S_{mn}, TPa^{-1}	p^E_{in}
11	−1.7 ± 0.15	−1.6	25.63	−0.195
12	−1.35 ± 0.08	−1.46	−14.85	−0.197
13	1.75 ± 0.23	1.73	−9.97	−0.059
31	−1.6 ± 0.15	−1.6	−9.97	−0.112
33	3.7 ± 0.37	3.7	37.21	0.039
14	−2.0 ± 0.8	−1.54	22.6 [4]	−0.005
41	−2.03 ± 0.07	−2.02	22.6 [4]	−0.007
44	−26.3 ± 0.9	−26.3	331.3	−0.078

3. The indicative surfaces and their stereographic projections

The analysis of spatial anisotropy of the photoelastic properties is based on the indicative surfaces and their stereographic projections. The corresponding method developed in [10] allows to describe both qualitatively and quantitatively the anisotropy of any physical effect in the crystals. We must mention that any ambiguity both in determination of piezo- or photoelastic constants as well as then in the constructing of the indicative surfaces can be removed if to use always the same coordinate system, in particular the one, which was used for the determination of the piezooptic coefficients. In the photoelastic measurements it is important also to choose properly the positive directions of principal coordinate system. This problem has been already discussed in details [11–13]. The equations of the indicative surfaces of the photoelastic effect can be derived in a similar way as for piezooptic effect (see Refs. [3,11]). In the spherical coordinate system (θ, φ) these equations for BBO crystals get the form:

$$p'_{ii}(\theta,\varphi) = p_{11}\sin^4\theta + (p_{13} + p_{31} + 4p_{44})\sin^2\theta\cos^2\theta + p_{33}\cos^4\theta + 2(p_{14} + p_{41})\sin^3\theta\cos\theta\sin 3\varphi, \quad (3)$$

$$p'^{(i)}_{in}(\theta,\varphi) = p_{12}\sin^2\theta + p_{31}\cos^2\theta - 2p_{41}\sin\theta\cos\theta\sin 3\varphi, \quad (4)$$

$$p'^{(n)}_{in}(\theta,\varphi) = p_{12}\sin^2\theta + p_{13}\cos^2\theta - 2p_{14}\sin\theta\cos\theta\sin 3\varphi, \quad (5)$$

where $p'_{ii}(\theta,\varphi)$ is the indicative surface of the longitudinal photoelastic effect, $p'^{(i)}_{in}(\theta,\varphi)$ and $p'^{(n)}_{in}(\theta,\varphi)$ are the indicative surfaces of the transverse photoelastic effect for light polarization and mechanical deformation, respectively. Fig. 1(a)–(c) shows the indicative surfaces and their stereographic projections (d)–(f) for the longitudinal (p'_{ii} – a, d) and transverse ($p'^{(i)}_{in}$ – b, e; $p'^{(n)}_{in}$ – c, f) photoelastic effect in β-BaB_2O_4 crystals calculated using the Eqs. (3)–(5) and the data (p^E_{in}) presented in the Table 1. More details concerning the method used for a construction of these surfaces is described elsewhere [3,12]. The surfaces were built using the elaborated software by means of meridian and equatorial cross sections with further their projection on the plane. In order to lower shadowing the only upper part of these surfaces are pictured. Complete image of each surface can be represented through an imaginary reproduction relatively to the centre of the coordinate system.

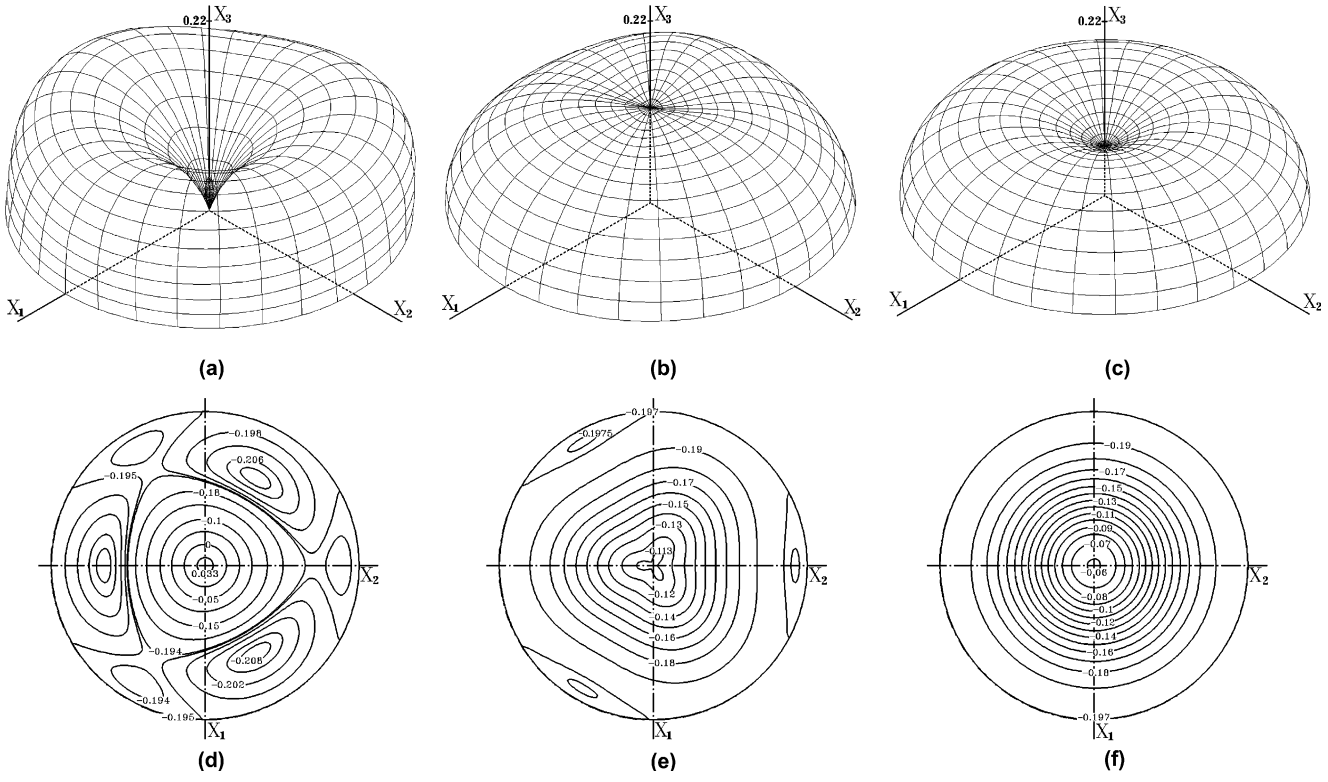

Fig. 1. The indicative surfaces (a)–(c) and their stereographic projections (d)–(f) for longitudinal (p'_{ii} – a, d) and transverse ($p'^{(i)}_{in}$ – b, e; $p'^{(n)}_{in}$ – c, f) photoelastic effect in β-BaB_2O_4 crystals.

Considering the indicative surfaces as a function of $f(\theta,\varphi)$ (i.e. $f(\theta,\varphi) = p'_{ii}(\theta,\varphi)$, $p'^{(i)}_{in}(\theta,\varphi)$ or $p'^{(n)}_{in}(\theta,\varphi)$) we have calculated the anisotropy power according to the relationship [3]

$$\eta = (V_{sp} - |V^+ - V^-|)100\%/V_{sp}, \quad (6)$$

where $V_{sp} = 4\pi|f_{extr}|^3/3$ is a sphere volume with radius $|f_{extr}| = \max(|f_{min}|, |f_{max}|)$, V^+ and V^- are the volumes of positive and negative parts of surface, respectively. The anisotropy power defined in such way gives $\eta = 0\%$ when the indicative surface is a sphere whereas if $V^+ = V^-$ then the effect has the maximum anisotropy power, i.e. $\eta = 100\%$.

4. Spatial anisotropy of the photoelastic effect

The longitudinal photoelasic effect in BBO crystals (Fig. 1(a)) is characterized by the pronounced anisotropy including the sign inversion. For comparison the anisotropy of transverse photoelasic effect is less pronounced with the lack of the sign inversion (Fig. 1(b) and (c)). At the same time, the anisotropy power η (see Table 2) calculated according to the Eq. (6) appear to be a bit larger for the indicative surface of the transverse effect $p'^{(n)}_{in}(\theta,\varphi)$.

In comparison to the piezooptic effect (see paper [3]) the indicative surfaces of the photoelastic effect have essentially smaller (of about two times) value of η, namely for $p'^{(i)}_{in}(\theta,\varphi)$ and $p'^{(n)}_{in}(\theta,\varphi)$ surfaces. In addition they have much simpler shape and no sign inversion. The latter fact can be explained by the small values of the photoelastic constants p_{14} and p_{41} as well as by the same signs of photoelastic constants p_{12}, p_{13} and p_{31}.

Several other features regarding the symmetry follow from the detailed analysis the indicative surfaces in the Fig. 1. The surfaces $p'_{ii}(\theta,\varphi)$ and $p'^{(i)}_{in}(\theta,\varphi)$ clearly do not have a rotation symmetry, what indeed is consistent with the German's theorem [14]. In fact, these surfaces

Table 2
Extreme values and anisotropy power for the indicative surfaces of the photoelastic effect in BBO crystals (see Fig. 1)

Indicative surface	Maximal value			Minimal value			Anisotropy power		
	Magnitude	θ	φ	Magnitude	θ	φ	V_{sp}, (unit)^3	$\lvert V^+ - V^-\rvert$, (unit)^3	η,%
p'_{ii} (Fig. 1(a))	0.039	0°	–	−0.209	67°	30°, 150° or 270°	0.038	0.023	39
$p'^{(i)}_{in}$ (Fig. 1(b))	−0.111	5°	30°, 150° or 270°	−0.198	85°	90°, 210° or 330°	0.032	0.021	34
$p'^{(n)}_{in}$ (Fig. 1(c))	−0.059	2°	30°, 150° or 270°	−0.197	88°	90°, 210° or 330°	0.032	0.017	47

Table 3
Anisotropy of the acoustooptical properties in BBO crystals (as for $T = 20\,^{\circ}C$ and $\lambda = 0.6328\,\mu m$ light wave length)

Sample geometry no.	Type of diffraction	Polarization of optic wave				Refractive index	Acoustic wave				Mode[a]	Velocity V, 10^3 m/s	Effective photoelastic constant p_{ef}	Figure of merit		
		Incidented light $\mathbf{i}_\mu$		Diffracted light $\mathbf{i}_\nu$			Propagation **a**		Polarization **f**					$M \times 10^{15}$, s^3/kg	$M' \times 10^8$, m^2s/kg	$M'' \times 10^{11}$, ms^2/kg
		θ	φ	θ	φ		θ	φ	θ	φ						
1	Isotropic	[100]		[100]		$n_\mu = n_\nu = n_0$	[100]		[100]		L	5.24	$p_{11} = -0.195$	1.48	6.8	1.29
2	Isotropic	[100]		[100]		$n_\mu = n_\nu = n_0$	[010]		89°	90°	QL	5.24	$\tilde{p}_{12} = -0.197$	1.51	6.9	1.32
3	Isotropic	[100]		[100]		$n_\mu = n_\nu = n_0$	[001]		[001]		L	3.73	$p_{13} = -0.059$	0.38	0.87	0.23
4	Isotropic	[010]		[010]		$n_\mu = n_\nu = n_0$	[100]		[100]		L	5.24	$p_{21} = -0.197$	1.51	6.9	1.32
5	Isotropic	[001]		[001]		$n_\mu = n_\nu = n_e$	[100]		[100]		L	5.24	$p_{31} = -0.112$	0.31	1.34	0.26
6	Isotropic	[001]		[001]		$n_\mu = n_\nu = n_e$	[001]		[001]		L	3. 72	$p_{33} = 0.039$	0.11	0.23	0.06
7	Isotropic	[010]		[010]		$n_\mu = n_\nu = n_0$	[010]		89°	90°	QL	5.24	$\tilde{p}_{22} = -0.195$	1.48	6.8	1.29
8	Isotropic*	64°	30°	64°	30°	$n_\mu = n_\nu = 1.642$	64°	30°	76°	30°	QL	4.82	$\tilde{p}_{ef} = \mathbf{-0.207}$	1.86	7.1	1.47
9	Isotropic**	56°	30°	56°	30°	$n_\mu = n_\nu = 1.628$	56°	30°	69°	30°	QL	4.58	$\tilde{p}_{ef} = -0.204$	**1.93**	6.6	1.44
10	Isotropic	[100]		[100]		$n_\mu = n_\nu = n_0$	[010]		1°	−90°	QT	0.92	$\tilde{p}_{14} = -0.002$	0.015	0.002	0.002
11	Isotropic	[100]		[100]		$n_\mu = n_\nu = n_0$	[001]		[010]		T	0.93	$p_{14} = -0.005$	0.15	0.022	0.024
12	Isotropic*	26°	30°	26°	30°	$n_\mu = n_\nu = 1.571$	26°	30°	121°	30.1°	QT	1.56	$\tilde{p}_{ef} = \mathbf{0.094}$	6.1	2.34	1.5
13	Isotropic**	21°	30°	21°	30°	$n_\mu = n_\nu = 1.564$	21°	30°	114°	30.1°	QT	1.40	$\tilde{p}_{ef} = -0.089$	**6.3**	1.94	1.39
14	Anisotropic	[010]		[001]		$n_\mu = n_0$; $n_\nu = n_e$	[100]		[100]		L	5.24	$p_{41} = -0.007$	0.002	0.007	0.001
15	Anisotropic*	[001]		[010]		$n_\mu = n_e$; $n_\nu = n_0$	41°	−90°	52°	−90°	QL	4.11	$\tilde{p}_{ef} = \mathbf{0.082}$	0.40	1.1	0.26
16	Anisotropic**	[001]		[010]		$n_\mu = n_e$; $n_\nu = n_0$	35°	−90°	44°	−90°	QL	3.96	$\tilde{p}_{ef} = -0.079$	**0.44**	1.1	0.28
17	Anisotropic	[010]		[001]		$n_\mu = n_0$; $n_\nu = n_e$	[001]		[010]		T	0.93	$p_{44} = -0.078$	30	4.2	4.5
18	Anisotropic	[010]		[001]		$n_\mu = n_0$; $n_\nu = n_e$	[010]		1 °	−90°	QT	0.92	$\tilde{p}_{44} = -0.079$	34	4.6	5.0
19	Anisotropic*	4°	90°	90°	180°	$n_\mu = 1.551$; $n_\nu = n_0$	4°	90°	90°	180°	QT	0.90	$\tilde{p}_{ef} = \mathbf{-0.079}$	**36**	4.7	5.2
20	Anisotropic**	4°	210°	90°	120°	$n_\mu = 1.551$; $n_\nu = n_0$	90°	120°	9.8°	30°	QT	0.88	$\tilde{p}_{ef} = -0.078$	**40**	5.0	5.7

(*) and (**)-calculated maximum values for effective photoelastic constants p_{ef} and figures of merit M respectively; $n_0 = 1.550$ and $n_e = 1.667$ are the ordinary and extraordinary refractive indices, respectively.

[a] L (QL) and T (QT) are the pure (quasi-) longitudinal and pure (quasi-) transverse acoustic waves, respectively, symbol "$\sim$" over the notations p_{in} indicates on the effective but not pure photoelastic constant.

can be described by the point group of symmetry 3m: a threefold axis and three symmetry planes, which are normal to the (X_1, X_2) isotropic plane. This corresponds to well-known Neumann principle [15]. At the same time the surface $p_{in}^{\prime(n)}(\theta,\varphi)$ looks like to have the rotation symmetry although the Eq. (5) indeed again predicts the same point symmetry, i.e. 3m. This can be explained by very small magnitude of photoelastic constant p_{14} thereby the corresponding weak surface distortions are practically not seen in the Fig. 1(g).

As the common feature for all the indicative surfaces of both piezooptic and photoelastic effects is the existence of their circular cross section in the plane normal to the optical axis. It means that at a given deformation, the induced changes of the refractive indices remain constant at any angular position of the light polarization or the direction of the applied uniaxial deformation in the isotropic (X_1, X_2) plane. This appears to be actual for both longitudinal and transverse photoelastic effects.

The extreme values of $p_{in}^{\prime(n)}(\theta,\varphi)$ surface are not shown on the stereographic projection (Fig. 1(g)) since they cannot be determine by means of the Wulff network. However, they as well as the extreme values of $p_{in}^{\prime(i)}(\theta,\varphi)$ surface can be found numerically by applying the conditions $\partial p'/\partial\theta = 0$ and $\partial p'/\partial\varphi = 0$. Such calculations give the values of about -0.111 and -0.059 together with the following angular coordinates $\theta = 0.5\arctan(2p_{41}/(p_{12}-p_{31})) \approx 5°$, $\varphi = 30° \pm 120° \cdot n$, where $n = 0,1,2,\ldots$ and $\theta = 0.5\arctan(2p_{14}/(p_{12}-p_{13})) \approx 2°$, $\varphi = 30 \pm 120° \cdot n$ for the indicative surfaces $p_{in}^{\prime(i)}(\theta,\varphi)$ and $p_{in}^{\prime(n)}(\theta,\varphi)$, respectively (see Table 2). All the rest of extreme values presented in Table 2 were obtained from the numerical analysis or by using the calculated stereographic projections (Fig. 1(d) and (e)) by means of the Wulff network. A zero-isoline, which is presented on the stereographic projection for the longitudinal effect only (see Fig. 1(d)), defines the set of directions when the photoelastic effect is absent.

5. Figure of merit

The magnitude of effective photoelastic constants defines the efficiency of acoustooptical diffraction. Table 3 presents the effective photoelastic constants p_{ef} calculated according to [6,9]

$$p_{ef} = \vec{i}_\mu \vec{i}_\nu \hat{p} \vec{a} \vec{f}_q \tag{7}$$

where μ, $\nu = 1,2$; $q = 1,2,3$; $\vec{i}_\mu$ and $\vec{i}_\nu$ are the orts of the polarization directions for incident and diffracted light, respectively; $\vec{a}$ and $\vec{f}_q$ are the orts of the propagation and polarization directions for acoustic wave, respectively; $\hat{p}$ is the photoelastic tensor. If $\mu = \nu$ one deals with the isotropic acoustooptic diffraction otherwise (i.e. if $\mu \neq \nu$) the anisotropic type of diffraction is considered. According to [9], the symbol q defines the polarization of acoustic wave. The cases when $q = 1$ or 2 correspond to a slow or fast transverse acoustic waves, respectively, whereas the case when $q = 3$ corresponds to the longitudinal acoustic wave.

Table 3 presents also the figures of merit characteristics of BBO crystals calculated as [6,9]: $M = p_{ef}^2 \tilde{n}^6/\rho V^3$, $M' = p_{ef}^2 \tilde{n}^7/\rho V$ and $M'' = p_{ef}^2 \tilde{n}^7/\rho V^2$. Here $\tilde{n} = \sqrt{n_\mu n_\nu}$, where n_μ and n_ν are the refractive indices of the incident and diffracted light, ρ is the crystal density, V is acoustic wave velocity. In Table 3 the polarizations of optic and acoustic waves are chosen thus that the effective constant of p_{ef} coincides with the photoelastic constant p_{in}. The exceptions concern the constants p_{12} and p_{22} (see sample geometries No. 2 and No. 7) since the acoustic waves propagating in [0 1 0]-direction are either quasi-longitudinal (QL) or quasi-transverse (QT). For this reason we obtain the different values for p_{14} and $\tilde{p}_{14}$ (sample geometries No. 10 and No. 11) or p_{44} and $\tilde{p}_{44}$ (sample geometries No. 17 and No. 18) for the acoustic waves propagating along the directions [0 0 1] (with the polarization ‖[0 1 0]) and [0 1 0] (with the polarization ‖[0 0 1]).

The geometries of the acoustooptical interaction with the maximum magnitudes of the effective elastooptic coefficient p_{ef} (marked in the Table 3 as *) and figure of merit M (marked as **) for different types of acoustooptic diffraction have been determined within the numerical optimization procedure. According to [9] during the computer simulations we considered only the case when the propagation directions for optic and acoustic waves are orthogonal.

By analyzing the data of Table 3 we see that the most efficient acoustooptic interaction in BBO crystals occur for isotropic diffraction (sample geometry No. 13, $M = 6.3 \times 10^{-15}\,s^3/kg$) and for anisotropic diffraction (sample geometry No. 20, $M = 40 \times 10^{-15}\,s^3/kg$). The latter case is the most attractive speaking about the

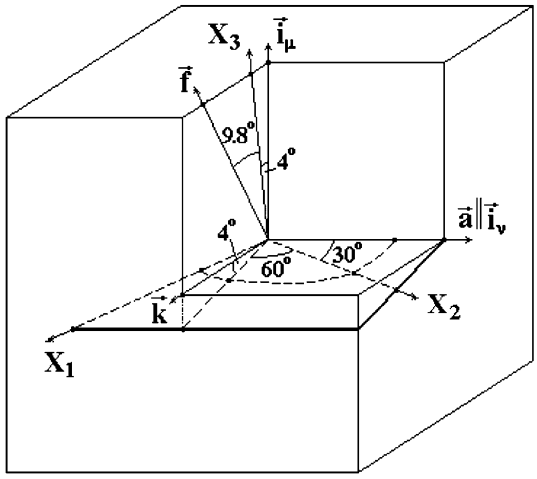

Fig. 2. The sample geometry giving the maximum figure of merit M in β-BaB_2O_4 crystals (X_1, X_2, X_3 is the crystallophysical reference system; $\vec{k}$ is the direction of light propagation).

application aspects of BBO crystals in acoustooptic devices such as modulators and deflectors. In details this geometry is shown in the Fig. 2. One should remember that BBO are rather strong radiation-steady crystals [16]. For this reason they may be considered as the perspective acoustooptical materials for application in optical systems with superpower laser irradiation.

6. Conclusion

Paper deals with the spatial anisotropy of the photoelastic properties in the β-BaB_2O_4 crystals. For this reason the indicative surfaces and stereographic projections of longitudinal and transverse photoelastic effects were constructed. We have performed the numerical analysis of the indicative surfaces in order to find the geometries with the strongest photoelastic interaction. The anisotropy power is also determined. Having the complete photoelastic tensor we have calculated the effective photoelastic constant p_{ef} and the efficiency of isotropic and anisotropic diffractions (figure of merit M) for different sample geometries of acoustooptical interactions. The most optimal sample geometries were determined within the computer simulations based on the optimization procedure, namely we have found the sample geometries characterizing by maximal efficiencies of the isotropic ($M = 6.3 \times 10^{-15}\,s^3/kg$) and anisotropic ($M = 40 \times 10^{-15}\,s^3/kg$) diffractions. Taking into account that BBO is known as a rather strong radiation-steady crystals it may be considered as new efficient acoustooptical material for applications in optical systems with superpower laser irradiation.

Acknowledgment

This work has been supported by STCU-program (proj. N# 1712 and N# 3222).

References

[1] C. Chen, Yi. Wu, K. Li, J. Cryst. Growth 99 (1990) 790.
[2] C. Chen, Y. Fan, R.C. Eckord, R.L. Byer, Proceedings of SPIE 68 (1997) 12.
[3] A.S. Andrushchak, V.T. Adamiv, O.M. Krupych, I.Yu. Martynyuk-Lototska, Ja.V. Burak, R.O. Vlokh, Ferroelectrics 238 (2000) 299.
[4] A.S. Andrushchak, Ya.V. Bobitski, M.V. Kaidan, V.T. Adamiv, Y.V. Burak, B.G. Mytsyk, Opt. Appl. 33 (2003) 345.
[5] A.S. Andrushchak, Ya.V. Bobitski, M.V. Kaidan, B.G. Mytsyk, A.V. Kityk, W. Schranz, Opt. Laser Technol., in press.
[6] T. Narasimhamurty, Photoelastic and electrooptic properties of crystals, Plenum Press, New-York, London, 1981.
[7] L. Bohaty, J. Liebertz, Z. Kristallogr. 192 (1990) 91.
[8] D. Eimeri, L. Devis, S. Velsko, E.K. Grahow, A. Zalkin, J. Appl. Phys. 62 (1987) 1968.
[9] V.I. Balakshyj, V.N. Parygin, L.E. Chirkov, Fizicheskiye osnovy akustooptiki, Izd. Radio i Svjat, Moscow 1985.
[10] Yu.I. Sirotin, M.P. Shaskolskaya, Osnovy kristalofiziki, Nauka, Moscow 1975.
[11] B.G. Mytsyk, Ya.V. Pryriz, A.S. Andrushchak, Cryst. Res. Technol. 26 (1991) 931.
[12] B.G. Mytsyk, A.S. Andrushchak, Crystallogr. Rep. 41 (1996) 1001.
[13] B.G. Mytsyk, A.S. Andrushchak, Ukr. Phys. J. 38 (1993) 1015.
[14] V.L German, Dokl. Akad. Nauk SSSR 48 (1945) 95.
[15] J.F. Nye, Physical Properties of Crystals, Clarendon Press, Oxford, 1992.
[16] C. Chen, B. Wu, A. Jiang, G. You, Scientia Sinica Ser. B 28 (1985) 235.